Dipartimento di Scienze Matematiche
Università Politecnica delle Marche
Via Brecce Bianche 1
I-60131 Ancona, Italy

Quaderno N. 3 - Aprile 2003

Lucio Demeio
Paolo Bordone and **Carlo Jacoboni**

Multi-band, non-parabolic Wigner-function approach to electron transport in semiconductors.

Multi-band, non-parabolic Wigner-function approach to electron transport in semiconductors.

Lucio Demeio
Dipartimento di Scienze Matematiche
Università Politecnica delle Marche
Via Brecce Bianche 1
I-60131 Ancona, Italy
Paolo Bordone and **Carlo Jacoboni**
INFM - National Research Center on
nanoStructures and bioSystem at Surfaces (S^3) and
Dipartimento di Fisica
Università di Modena e Reggio Emilia
Via Campi 213/A
I-41100 Modena, Italy

April 4, 2003

Abstract

In this work, we introduce a multiband transport model for quantum electron transport in semiconductors following the Wigner-function approach. By using the Bloch-Floquet decomposition of the density matrix, we obtain the Bloch-Floquet projections of the Wigner function and derive their evolution equations for energy bands of arbitrary shape. The equations of the model are very general and allow, in principle, the investigation of quantum processes in which interband transitions and/or non-parabolicity effects may occur. Finally, we present numerical applications for some particulare cases, in which the numerical solution can be obtained easily.

1 Introduction

The Wigner-function approach to quantum electron transport in semiconductors is widely used to describe the properties of electronic devices such as the Resonant Tunneling Diode (RTD) and others [1, 2, 3, 4, 5]. By making use of phase space concepts, it presents a close analogy to the classical Boltzmann-equation approach and therefore many of the analytical and numerical techniques commonly used for the Boltzmann equation can be adapted to the Wigner function. The physical picture offered by the Wigner-function approach also remains closer to the classical one than the picture offered by other quantum statistical approaches to electron transport, such as the density-matrix approach [6, 7, 8] and the Green's-function approach [9, 10, 11]. In addition, when dealing with space dependent problems in finite domains, it is always difficult to devise the correct boundary conditions to be imposed; because of the analogy with the classical Boltzmann equation, this difficulty is more easily overcome with the Wigner-function approach, since one can rely on imposing classical boundary conditions in a region sufficiently far from the quantum region, where classical effects dominate [3]. Finally, adding collisions to the model equations that govern the evolution of the Wigner function is less complicated than including collisions into the other statistical models of quantum transport [2].

The applications of the Wigner-function formalism to semiconductor devices have been limited, until now, to the description of the conduction electrons that populate the region near the minimum of the conduction band. This leads to the single-band model in conjunction with the parabolic-band approximation. Under these conditions, conduction electrons can be considered as particles having an effective mass related to the curvature of the energy band function near the minimum. The evolution equation for the Wigner function of the conduction electrons then becomes the evolution equation for free particles with an effective mass. This allows the inclusion of any fields (barriers or bias) by means of the standard scattering integral (pseudodifferential [1, 12]) operator.

In the case of devices in which interband transitions or non-parabolicity effects may occur, the single-band, effective mass approximation is not satisfactory. A correctly defined Wigner function for these phenomena should include the populations of all bands involved in the transport processes and the evolution equation that governs the time dependence of the Wigner function should take into account possible non-parabolicity effects. In this work, we remove the single-band approximation and the parabolic band approximation, by introducing a Wigner function which includes the populations of all energy bands and derive an evolution equation which allows for energy bands of arbitrary shape. The resulting equations provide an exact model for the description of collisionless electron transport in semiconductors without the single-band and the parabolic band approximations. We also discuss the derivation of the parabolic band approximation starting from the exact equations. On this topic, some results have already appeared in the literature for particular cases. In absence of external fields, the evolution equations are a generalization of an earlier result for a single band by Markowich, Mauser and Poupaud [13, 14]. A statistical description of multiband transport was formulated by Krieger and Iafrate [15, 16] by making use of accelerated Bloch states in a model based on the density matrix. A two-band kinetic model without external fields was developed by Kuhn and Rossi [17] and by Hess and Kuhn [18] for the description of semiconductor lasers. The Wigner-function formalism has also been used by Buot and Jensen [19, 20, 21, 22] to formulate multi-band models within the framework of the Lattice-Weyl transform, in which a non-canonical definition of the Wigner function, based on a discrete Fourier Transform, was introduced.

Our multi-band model adopts a straightforward expansion of the wave functions in Bloch states and a Bloch-state representation of the density matrix. Probably, it is the most general way of formulating a multi-band model with the Wigner-function approach; other formulations, such as envelope functions and the Kane model, have recently been explored in the literature [23, 24].

Parts of this work have already been presented and published [25, 26, 27].

Here, we intend to present the comprehensive work in full detail and add some newer developments. The paper is organized as follows. In Section 2 we briefly recall the structure of the Hamiltonian and the energy eigenvalues and eigenfunctions for a periodic potential; in Section 3 the multi-band Wigner function is introduced; in Section 4 we derive the evolution equation for the multi-band Wigner function; in Section 5 some simplified models are presented and in Section 6 we show some numerical applications.

2 The Hamiltonian and the Bloch representation

We consider an ensemble of electrons moving in a semiconductor crystal. For simplicity, we consider a one-dimensional case. The quantum dynamics is generated by the Hamiltonian

$$H = H_0 + V(x),$$

where $H_0 = p^2/2m + V_p(x)$ is the single electron Hamiltonian, which contains the kinetic energy and the periodic potential $V_p(x)$, and which will be called the "free Hamiltonian". Also, $p = -i\hbar\partial/\partial x$ is the momentum operator, m is the electron mass, $\hbar$ is Plank's constant and $V(x)$ is the potential due to external fields, such as barriers or bias. Let $\Psi_m(x,k)$ be the eigenfunctions and $\epsilon_1(k)$, $\epsilon_2(k)$, ..., $\epsilon_{m-1}(k)$, $\epsilon_m(k)$, ..., the (real) eigenvalues of the free Hamiltonian H_0,

$$H_0\Psi_m(x,k) = \epsilon_m(k)\Psi_m(x,k). \tag{1}$$

($H_0|m,k> = \epsilon_m(k)|m,k>$ in Dirac's notation). Here, $m \in \mathbf{N}$ is the band index and k is the crystal momentum, with $k \in B$ and B the Brillouin zone. The eigenfunctions $\Psi_m(x,k)$ are given by the Bloch functions

$$< x|mk > \equiv \Psi_m(x,k) = e^{ikx}u_{mk}(x) \tag{2}$$

and form a complete orthonormal set. Here, $u_{mk}(x)$ is the periodic part of the Bloch function for the m-th band and the states $\{|mk>\}$, $m \in \mathbf{N}$, $k \in B$ are the Bloch states. We have that $u_{mk}(x+a) = u_{mk}(x)$, with a the lattice period, and

$$e^{ik\mu} < x|mk > = < x+\mu|mk > \tag{3}$$

$\forall \mu \in L$, with L the direct lattice. The completeness and orthogonality of the Bloch states are expressed by the relations

$$\sum_m \int_B dk < x|mk >< mk|x' >= \delta(x - x'),$$

and

$$\int_{\mathbf{R}} dx < mk|x >< x|nk' >= \delta_{mn}\delta(k - k').$$

For the one-dimensional model considered here, we have that

$$\int_B dk = \int_{-\pi/a}^{\pi/a} dk.$$

The functions $\epsilon_m(k)$ are the energy bands of the material and are real functions, periodic in the crystal momentum k with period $2\pi/a$. They can be expanded in Fourier series,

$$\epsilon_m(k) = \sum_{\mu \in L} \widehat{\epsilon}_m(\mu) e^{ik\mu}, \tag{4}$$

with $\widehat{\epsilon}^*_m(\mu) = \widehat{\epsilon}_m(-\mu)$ from the reality condition of the energy bands.

3 The multi-band Wigner function

The main quantity of a quantum statistical description of an ensemble of electrons in phase space is the Wigner function, which is defined by a suitable Fourier transformation of the density matrix [1]. Let $\rho(r,s) =< r|\rho|s >$ be the single particle density matrix in the space representation. Then, the corresponding single-electron Wigner function [1] is defined by

$$f(x,p) = \int d\eta < x + \frac{\eta}{2}|\rho|x - \frac{\eta}{2} > e^{-ip\eta/\hbar}, \tag{5}$$

together with its inverse

$$< r|\rho|s >= \frac{1}{2\pi\hbar} \int dp f\left(\frac{r+s}{2}, p\right) e^{ip(r-s)/\hbar}. \tag{6}$$

Usually, $x = (r+s)/2$ is identified with a center of mass variable and $\eta = r - s$ with a relative position variable.

In general, an electron in the crystal will be found in a statistical superposition of Bloch states belonging to different energy bands. In many situations, however, it is a good approximation to consider only the electron population of a single band, usually the conduction band, in which case the Wigner function describes only that electron population. This is the case, for example, of the RTD; for this device, only the conduction electrons contribute significantly to the flow of current and a transport model based on the single band approximation is sufficient to calculate the $I-V$ curves of the device with very good accuracy [2]. If we wish to use the Wigner-function approach to study situations in which interband transitions occur, however, the single-band approximation is no longer satisfactory and a more general theory is needed. These situations include, for example, Zener tunneling and resonant interband tunneling diodes (RITD [28]); also, scattering processes could induce interband transitions and during a scattering event an electron may be in a superposition of Bloch states belonging to different bands. For a quantum statistical description of these phenomena, the Wigner function has to contain the information about the electron populations of all energy bands and their dynamics.

A suitable partition of the Wigner function among the energy bands is obtained by using Bloch states and the matrix elements of the density operator in the Bloch-state representation. By using the completeness of the Bloch states $\{|mk>\}$ in equation (5), the Wigner function can be written as a double sum of contributions from all energy bands:

$$f(x,p) = \sum_{mn} f_{mn}(x,p), \tag{7}$$

where

$$f_{mn}(x,p) = \int_{B^2} dk dk' \rho_{mn}(k,k') \int d\eta < x + \frac{\eta}{2}|mk >< nk'|x - \frac{\eta}{2} > e^{-ip\eta/\hbar} \tag{8}$$

and

$$\rho_{mn}(k,k') =< mk|\rho|nk' > . \tag{9}$$

The functions f_{mn} are the projections of f onto the Floquet band subspaces.

Equation (8) can be written in a more compact form, as the result of a projection operator $\mathcal{P}_{mn}$ acting on the Wigner function f, $(\mathcal{P}_{mn}f)(x,p) =$

$f_{mn}(x,p)$. By introducing the coefficients

$$\Phi_{mn}(k,k',x,p) = \int d\eta < x + \frac{\eta}{2}|mk >< nk'|x - \frac{\eta}{2} > e^{-ip\eta/\hbar}, \qquad (10)$$

and after substituting into (8), we have:

$$f_{mn}(x,p) = \int_{B^2} dkdk'\Phi_{mn}(k,k',x,p)\rho_{mn}(k,k'). \qquad (11)$$

(the summation over repeated indeces is not used). It can be easily seen that the coefficients (10) obey the following relations:

$$\frac{1}{2\pi\hbar}\int\int \Phi_{mn}(k,k',x,p)\,dxdp = \delta_{mn}\delta(k-k') \qquad (12)$$

$$\int\int \Phi_{mn}(k_1,k_2,x,p)\Phi_{m'n'}(k_1',k_2',x,p)\,dxdp =$$
$$= \delta_{mm'}\delta_{nn'}\delta(k_1-k_1')\delta(k_2-k_2') \qquad (13)$$

The elements $\rho_{mn}(k,k')$ of the density matrix in the Bloch-state representation can be written in terms of the Wigner function by using (6):

$$\rho_{mn}(k,k') =< mk|\rho|nk' >= \int\int drds < mk|r >< r|\rho|s >< s|nk' >=$$
$$= \int\int drds < mk|r >< s|nk' > \frac{1}{2\pi\hbar}\int dpf\left(\frac{r+s}{2},p\right)e^{ip(r-s)/\hbar} =$$
$$= \frac{1}{2\pi\hbar}\int\int \Phi^*_{mn}(k,k',x,p)f\,(x,p)\;dxdp,$$

where the change of variables $x = (r+s)/2$, $\eta = r-s$ has been used in the integration over space. Finally, we obtain:

$$f_{mn}(x,p) = \frac{1}{2\pi\hbar}\int\int dx'dp'W_{mn}(x,p,x',p')f\,(x',p') \equiv (\mathcal{P}_{mn}f)(x,p). \qquad (14)$$

where the integral kernel W_{mn} is given by

$$W_{mn}(x,p,x',p') = \int_{B^2} dkdk'\Phi_{mn}(k,k',x,p)\Phi^*_{mn}(k,k',x',p'). \qquad (15)$$

Equation (14) defines the linear integral operator $\mathcal{P}_{mn}$, with the kernel W_{mn}, which yields the projections f_{mn} from the total Wigner function f.

The functions f_{mn} and the coefficients $\rho_{mn}(k',k'')$ are similar to the ones introduced in [4, 29, 30].

The macroscopic quantities such as particle density, current and energy, are also expressed as a sum of band terms. It can be shown that only the diagonal terms contribute to the total number of particles, that is

$$\int\int f(x,p)\,dx\,dp = \sum_m \int\int f_{mm}(x,p)\,dx\,dp,$$

which follows from the fact that $\int\int W_{mn}(x,p,x',p')\,dx\,dp = 0$ for $m \neq n$ because of equation (12).

4 General evolution equations

The time evolution of the Wigner function is given by the sum of the time evolutions of the band projections,

$$i\hbar\frac{\partial f}{\partial t}(x,p,t) = \sum_{mn} i\hbar\frac{\partial f_{mn}}{\partial t}(x,p,t),$$

and it must follow from the Liouville-von Neumann time evolution equation for the density matrix,

$$i\hbar\frac{\partial \rho}{\partial t} = [H,\rho]. \tag{16}$$

We analyze separately the contribution to the time evolution of the Wigner function due to the free Hamiltonian H_0, and the contribution due to the external potential V,

$$\frac{\partial \rho}{\partial t} = \left(\frac{\partial \rho}{\partial t}\right)_0 + \left(\frac{\partial \rho}{\partial t}\right)_V, \tag{17}$$

and

$$\frac{\partial f}{\partial t} = \left(\frac{\partial f}{\partial t}\right)_0 + \left(\frac{\partial f}{\partial t}\right)_V. \tag{18}$$

Here, $i\hbar(\partial\rho/\partial t)_0 = [H_0,\rho]$ and $i\hbar(\partial\rho/\partial t)_V = [V,\rho]$.

We begin by considering the time evolution of the Wigner function due to the free Hamiltonian. From equation (11) we have:

$$i\hbar\left(\frac{\partial f_{mn}}{\partial t}\right)_0(x,p,t) = \int_{B^2} dk\,dk'\,i\hbar\left(\frac{\partial \rho_{mn}}{\partial t}\right)_0(k,k',t)\Phi_{mn}(k,k',x,p), \tag{19}$$

where

$$i\hbar \left(\frac{\partial \rho_{mn}}{\partial t} \right)_0 (k,k',t) =< mk|[H_0,\rho]|nk >= [\epsilon_m(k) - \epsilon_n(k')]\rho_{mn}(k,k',t).$$

By substituting the above expression into equation (19) and by using equation (4) we then have:

$$\begin{aligned} & i\hbar \left(\frac{\partial f_{mn}}{\partial t} \right)_0 (x,p,t) = \\ & \quad = \int_{B^2} dkdk' \Phi_{mn}(k,k',x,p)[\epsilon_m(k) - \epsilon_n(k')]\rho_{mn}(k,k',t) = \\ & \quad = \int_{B^2} dkdk' \Phi_{mn}(k,k',x,p) \\ & \quad \sum_{\mu \in L} [\widehat{\epsilon}_m(\mu) e^{ik\mu} - \widehat{\epsilon}_n(\mu) e^{ik'\mu}]\rho_{mn}(k,k',t). \end{aligned} \tag{20}$$

In order to obtain an equation for f_{mn} in closed form, the right hand side of equation (20) must be rewritten in terms of f_{mn}. By using equations (10) and (11), and the relations
$e^{ik\mu} < x + \eta/2|mk >=< x + \mu + \eta/2|mk >$ and $e^{ik\mu} < mk|x - \eta/2 >=< mk|x - \mu - \eta/2 >$, which follow from equation (3), we find after some algebra:

$$\begin{aligned} & i\hbar \left(\frac{\partial f_{mn}}{\partial t} \right)_0 (x,p,t) = \\ & \quad = \sum_{\mu \in L} \left[\widehat{\epsilon}_m(\mu) f_{mn}(x + \frac{\mu}{2}, p, t) - \widehat{\epsilon}_n(\mu) f_{mn}(x - \frac{\mu}{2}, p, t) \right] e^{ip\mu/\hbar}. \end{aligned} \tag{21}$$

Equations (21) are the equations that govern the time evolution of the Floquet projections f_{mn} of the Wigner function for an ensemble of electrons moving in a semiconductor crystal in the absence of external fields and allowing for energy bands of arbitrary shape. These equations show that, in the absence of external fields, different bands remain dinamically uncoupled and each contribution to the Wigner function evolves independently. Equations (21) are a generalization to the multi-band case of an earlier result obtained by Markowich, Mauser and Poupaud [13, 14] for a single band. In the next Section, we shall relate these equations to the evolution equations in the parabolic-band approximation.

Next, we consider the time evolution of the Wigner function due to the external potential and which is given by

$$i\hbar \left(\frac{\partial f}{\partial t}\right)_V (x,p,t) = \int d\eta < x + \frac{\eta}{2}|[V,\rho]|x - \frac{\eta}{2} > e^{-ip\eta/\hbar}. \qquad (22)$$

We recall that the right hand side of equation (22) can be cast in the form [1, 13]

$$\int d\eta < x + \frac{\eta}{2}|[V,\rho]|x - \frac{\eta}{2} > e^{-ip\eta/\hbar} = (\Theta(\delta V)f)(x,p,t) \qquad (23)$$

where $\Theta(\delta V)$ is the pseudodifferential operator with symbol $\delta V(x,\eta) = V(x+\eta/2) - V(x-\eta/2)$,

$$(\Theta(\delta V)f)(x,p,t) = \int d\eta \delta V(x,\eta)\widehat{f}(x,\eta,t)e^{-ip\eta/\hbar}, \qquad (24)$$

and

$$\widehat{f}(x,\eta,t) = \frac{1}{2\pi\hbar}\int dp f(x,p,t)e^{ip\eta/\hbar}$$

is the Fourier transform of the Wigner function with respect to the momentum variable.

Equations (23) and (24) are very often written in a different form. By introducing the potential transfer function,

$$\mathcal{V}_W(x,p) = \frac{1}{2\pi\hbar}\int d\eta \delta V(x,\eta)e^{-ip\eta/\hbar}, \qquad (25)$$

we have

$$\begin{aligned}(\Theta(\delta V)f)(x,p,t) &= \int d\eta \delta V(x,\eta)\widehat{f}(x,\eta,t)e^{-ip\eta/\hbar} = \\ &= \frac{1}{2\pi\hbar}\int d\eta \delta V(x,\eta)\int dp' f(x,p',t)e^{-i(p-p')\eta/\hbar} = \\ &= \int dp' f(x,p',t)\mathcal{V}_W(x,p-p').\end{aligned}$$

The time evolution of f_{mn} due to the external potential can be obtained by acting on both sides of equation (22) with the operator $\mathcal{P}_{mn}$ defined in (14). From equation (23) we have:

$$\mathcal{P}_{mn}(\Theta(\delta V)f)(x,p,t) =$$

$$= \frac{1}{2\pi\hbar}\int\int dx'dp' W_{mn}(x,p,x',p')(\Theta(\delta V)f)(x',p',t) =$$
$$= \frac{1}{2\pi\hbar}\int\int dx'dp' W_{mn}(x,p,x',p')\int d\eta \delta V(x',\eta)\widehat{f}(x',\eta,t)e^{-ip'\eta/\hbar} =$$
$$= \frac{1}{2\pi\hbar}\int dx'\int dp' W_{mn}(x,p,x',p')e^{-ip'\eta/\hbar}\int d\eta \delta V(x',\eta)\widehat{f}(x',\eta,t) =$$
$$= \int\int dx'd\eta \widehat{W}_{mn}(x,p,x',-\eta)\delta V(x',\eta)\widehat{f}(x',\eta,t)$$

where

$$\widehat{W}_{mn}(x,p,x',\eta) = \frac{1}{2\pi\hbar}\int dp' W_{mn}(x,p,x',p')e^{ip'\eta/\hbar}$$

is the Fourier transform of W_{mn} with respect to the second momentum variable.

Finally, we obtain:

$$i\hbar\left(\frac{\partial f_{mn}}{\partial t}\right)_V(x,p,t) = \int\int dx'd\eta \widehat{W}_{mn}(x,p,x',-\eta)\delta V(x',\eta)\widehat{f}(x',\eta,t) \tag{26}$$

or, by using the potential transfer function (25),

$$i\hbar\left(\frac{\partial f_{mn}}{\partial t}\right)_V(x,p,t) =$$
$$\frac{1}{2\pi\hbar}\int dx'\int\int dp'dp'' W_{mn}(x,p,x',p'')f(x',p',t)\mathcal{V}_W(x',p''-p').$$

The full time evolution of the Floquet projection f_{mn} of the Wigner function, due both to the periodic potential of the crystal lattice and to the external potential, is obtained by adding the two contributions of equation (21) and equation (26):

$$i\hbar\frac{\partial f_{mn}}{\partial t} =$$
$$= \sum_{\mu\in L}\left[\widehat{\epsilon}_m(\mu)f_{mn}(x+\frac{\mu}{2},p,t) - \widehat{\epsilon}_n(\mu)f_{mn}(x-\frac{\mu}{2},p,t)\right]e^{ip\mu/\hbar} +$$
$$+\int\int dx'd\eta \widehat{W}_{mn}(x,p,x',-\eta)\delta V(x',\eta)\widehat{f}(x',\eta,t). \tag{27}$$

4.1 Quantum effects for linear and quadratic potentials

It is well known that, for particles having a parabolic energy-momentum dispersion relation and subject to linear and/or quadratic potentials, the

force term of the transport equation for the Wigner function, represented by a pseudodifferential operator, reduces to the classical differential term of the collisionless Boltzmann equation (the Vlasov equation). This fact is sometimes expressed by saying that, for linear and/or quadratic potentials, quantum effects do not appear in the dynamics. We now show that a similar property holds in the multiband case.

For both linear and quadratic potentials, the symbol δV of the pseudodifferential operator factors in the form

$$\delta V(x,\eta) = V(x+\eta/2) - V(x-\eta/2) = -F(x)\eta$$

where $F(x)$ is the force. For a linear potential, $V(x) = -Ex$, we have $F(x) = E$ and for a quadratic potential, $V(x) = \alpha x^2/2$, we have $F(x) = -\alpha x$. In either case, the standard pseudodifferential operator with the potential becomes the differential operator in momentum space of the classical Boltzmann equation:

$$\begin{aligned}\Theta(\delta V)f &= \int d\eta \delta V(x,\eta)\widehat{f}(x,\eta)e^{-ip\eta/\hbar} = -F(x)\int d\eta\eta\widehat{f}(x,\eta)e^{-ip\eta/\hbar} = \\ &= -F(x)\int d\eta\widehat{f}(x,\eta)\left(i\hbar\frac{\partial}{\partial p}\right)e^{-ip\eta/\hbar} = -i\hbar F(x)\frac{\partial f}{\partial p}.\end{aligned}$$

In the multiband case a more general result is obtained. From equation (26) we have:

$$i\hbar\left(\frac{\partial f_{mn}}{\partial t}\right)_V(x,p,t) = \mathcal{P}_{mn}(\Theta(\delta V)f)(x,p,t) = -i\hbar\mathcal{P}_{mn}\left(F\frac{\partial f}{\partial p}\right)(x,p,t) \tag{28}$$

which, in the case of a constant applied external field E, becomes

$$\left(\frac{\partial f_{mn}}{\partial t}\right)_V(x,p,t) = -E\mathcal{P}_{mn}\left(\frac{\partial f}{\partial p}\right)(x,p,t). \tag{29}$$

Note that, in general,

$$\mathcal{P}_{mn}\left(\frac{\partial f}{\partial p}\right) \neq \frac{\partial f_{mn}}{\partial p}$$

5 Derivation of simplified models from the exact general equations

Equations (27) are the most general time evolution equations that can be written for the Floquet projections of the multi-band Wigner function in presence of external fields and in absence of collisions. The action of the periodic potential is described by the first term, which contains the Fourier coefficients of the energy bands, and which reduces to the usual free-streaming operator in the parabolic-band approximation (see Section 5.1.1). The second term describes the action of the external potential. We note that, while the first term requires only the knowledge of the energy band functions, the second term requires the knowledge of the Bloch eigenfunctions of the material of interest. Therefore, the model equations (27) are very hard to solve in full generality in practical applications, and the derivation of a set of simplified models is desirable.

In the following subsections, we illustrate some of these simplified models; we divide them into two groups: models without external fields and models with external fields. Though external fields are present in most semiconductor applications, the models without external fields are useful to emphasize some of the theoretical aspects of the problem.

5.1 Models without external fields

5.1.1 Single band model in the parabolic band approximation

Here, we analyze the first term of equation (27) for a single band and show how it reduces to the free-streaming operator in the parabolic-band approximation. The single-band model with the parabolic band approximation is used to describe the electron population near the minimum of the conduction band. In the single band model, the total Wigner function f coincides with the Floquet projection of the conduction band and the sum over m and n in equation (7) collapses to a single term, say $m = n = 1$. Equation (21) with $m = n = 1$ then gives the time evolution of the Wigner function

of the conduction carriers for a band of arbitrary shape.

In the single band model, with the parabolic band approximation and in the absence of external potentials, the evolution equation for the Wigner function f is simply given by the free streaming part of the usual transport equation. That is, for a parabolic band $\epsilon(k)$ having a minimum at $k = 0$, we have

$$\frac{\partial f}{\partial t} + \frac{p}{m^*}\frac{\partial f}{\partial x} = 0,$$

where

$$m^* = \hbar^2 \left(\frac{\partial^2 \epsilon}{\partial k^2} \right)^{-1}_{k=0}$$

is the effective mass. If the energy band attains its minimum at $k = k^*$, the evolution equation is

$$\frac{\partial f}{\partial t} + \frac{p - \hbar k^*}{m^*}\frac{\partial f}{\partial x} = 0 \tag{30}$$

and

$$m^* = \hbar^2 \left(\frac{\partial^2 \epsilon}{\partial k^2} \right)^{-1}_{k=k^*}. \tag{31}$$

Equation (30) can be easily derived from equation (21) for a single band,

$$i\hbar \frac{\partial f}{\partial t}(x,p,t) = \sum_{\mu \in L} \widehat{\epsilon}(\mu) \left[f(x + \frac{\mu}{2}, p, t) - f(x - \frac{\mu}{2}, p, t) \right] e^{ip\mu/\hbar}, \tag{32}$$

where we have omitted the band index from the band energy function ($\epsilon(k)$ instead of $\epsilon_m(k)$) and from the band projection (f instead of f_{mn}) of the Wigner function. We shall also write $\partial f/\partial t$ for $(\partial f/\partial t)_0$ throughout this and the next Section. By expanding the nonlocal terms in the square brackets in a Taylor series about $\mu = 0$, we obtain:

$$i\hbar \frac{\partial f}{\partial t}(x,p,t) = -i \left[\frac{\partial \epsilon}{\partial k} \right]_{p/\hbar} \frac{\partial f}{\partial x} + i \frac{1}{4!} \left[\frac{\partial^3 \epsilon}{\partial k^3} \right]_{p/\hbar} \frac{\partial^3 f}{\partial x^3} + \ldots.$$

For a parabolic band, given by

$$\epsilon(k) = \epsilon(k^*) + \frac{\hbar^2 (k - k^*)^2}{2m^*}, \tag{33}$$

the derivatives of the energy band of third and higher order vanish identically, while

$$\left[\frac{\partial \epsilon}{\partial k}\right]_{p/\hbar} = \frac{\hbar}{m^*}(p - \hbar k^*),$$

and we obtain the evolution equation (30) for the Wigner function. Notice that the first non-parabolicity correction is proportional to the third derivative of the energy band and it involves the third partial derivative of the Wigner function with respect to the space variable.

5.1.2 Two-band band model in the parabolic band approximation

It is interesting to consider a simple two-band model in the parabolic band approximation to study the off-diagonal Floquet projections of the Wigner function, which arise in this case. In a two-band model, the Wigner function and its evolution equation are given by equations (7) and (21) where now $m = 0, 1$ and $n = 0, 1$. The Wigner function is given by the sum of four contributions, f_{00}, f_{01}, f_{10} and f_{11}. It can be seen easily from equations (10), (14) and (15) that $f_{01} = f_{10}^*$, while f_{00} and f_{11} are real. Each of the four contributions evolves according to equations (21). In the parabolic band approximation, the differential equations for f_{00} and f_{11} are identical to equation (30):

$$\frac{\partial f_{00}}{\partial t} + \frac{p - \hbar k_0}{m_0}\frac{\partial f_{00}}{\partial x} = 0 \tag{34}$$

$$\frac{\partial f_{11}}{\partial t} + \frac{p - \hbar k_1}{m_1}\frac{\partial f_{11}}{\partial x} = 0, \tag{35}$$

where m_0 and m_1 are the effective masses for band 0 and band 1 respectively and k_0 and k_1 are the values of the crystal momentum at which band 0 and band 1 attain their minimum. The evolution equations for f_{01} and $f_{10} = f_{01}^*$ have instead a different structure. A simple calculation shows that:

$$i\hbar\frac{\partial f_{01}}{\partial t} = \left\{\left[\epsilon_0(k_0) + \frac{(p - \hbar k_0)^2}{2m_0}\right] - \left[\epsilon_1(k_1) + \frac{(p - \hbar k_1)^2}{2m_1}\right]\right\} f_{01}(x, p) +$$
$$- \frac{i\hbar}{2}\left(\frac{p - \hbar k_0}{m_0} + \frac{p - \hbar k_1}{m_1}\right)\frac{\partial f_{01}}{\partial x} - \frac{1}{8}\left(\frac{\hbar^2}{m_0} - \frac{\hbar^2}{m_1}\right)\frac{\partial^2 f_{01}}{\partial x^2}. \tag{36}$$

which follows from equation (21) after expanding $f_{mn}(x \pm \eta/2, p, t)$ in Taylor series about $\mu = 0$ and using parabolic profiles for the two bands. By introducing the frequencies

$$\omega_{01} = (\epsilon_0(k_0) - \epsilon_1(k_1))/\hbar$$
$$\Omega_{01}(p) = \omega_{01} + (p - \hbar k_0)^2/(2m_0\hbar) - (p - \hbar k_1)^2/(2m_1\hbar)$$

and the new function

$$g_{01}(x, p, t) = f_{01}(x, p, t)e^{i\Omega_{01}(p)t},$$

equation (36) can be cast in the more elegant form

$$\frac{\partial g_{01}}{\partial t} + \frac{1}{2}\left(\frac{p - \hbar k_0}{m_0} + \frac{p - \hbar k_1}{m_1}\right)\frac{\partial g_{01}}{\partial x} - \frac{i\hbar}{8}\left(\frac{1}{m_0} - \frac{1}{m_1}\right)\frac{\partial^2 g_{01}}{\partial x^2} = 0. \quad (37)$$

Note that in the definition of the Wigner function (7) f_{01} and f_{10} appear only in the combination $f_{01} + f_{10}$, consistently with the Wigner function being real.

Equation (36) shows that the time evolution of f_{01} is given by three contributions: an oscillatory term, a free streaming term and a diffusive term with imaginary diffusion coefficient. The frequency of the oscillatory term, Ω_{01}, is proportional to the difference of the total energies of the particles of the two bands; the velocity of the free streaming term is an average of the relative velocities of the particle with respect to the two minima and the imaginary diffusion coefficient vanishes when the two effective masses are equal.

Equations (34), (35) and (37) completely describe the time evolution of all the components of the Wigner function in a two band model with the parabolic-band approximation and in the absence of external fields. Note that these evolution equations are uncoupled.

5.2 Models with external fields

5.2.1 Single-band model with arbitrary band profile

As in Subsection 5.1.1, the total Wigner function f coincides with the Floquet projection of the conduction band and the sum over m and n in

equation (7) collapses to a single term, say $m = n = 1$. The time evolution of the Wigner function is then obtained by considering equations (32), (22), (23) and (24) and is given by

$$i\hbar\frac{\partial f}{\partial t}(x,p,t) = \sum_{\mu\in L}\widehat{\epsilon}(\mu)\left[f(x+\frac{\mu}{2},p,t) - f(x-\frac{\mu}{2},p,t)\right]e^{ip\mu/\hbar} + \\ + \int d\eta\delta V(x,\eta)\widehat{f}(x,\eta,t)e^{-ip\eta/\hbar}. \tag{38}$$

and describes the evolution of the conduction carriers for a band of arbitrary shape. We shall illustrate this model with a numerical example in the next Section.

5.2.2 Multi-band model in the Luttinger-Kohn approximation

The Luttinger-Kohn model [31] considers the carrier populations near minima (or maxima) of the energy bands and it is therefore to be used in conjunction with the parabolic-band approximation. For the Bloch states near the minimum (or maximum) of the band, the periodic parts of the actual Bloch functions, $u_{mk}(x)$, are replaced with the set of functions $u_{mk_m}(x)$, i.e. the Bloch functions at the bottom (or top) of the band, here assumed at $k = k_m$. The functions $e^{ikx}u_{mk_m}(x)$ also form a complete set [31], and any wave function can be expanded in their basis. In this Section, we use the Luttinger-Kohn basis for expressing the Floquet projections of the Wigner function and for writing the evolution equations. The action of the free Hamiltonian is treated in the parabolic-band approximation.

If the $m-$th band has an extremum at $k = k_m$, we can approximate

$$< x|mk > \approx u_{mk_m}(x)e^{ikx}. \tag{39}$$

Since the functions $u_{mk_m}(x)$ are periodic functions with period a, we can introduce their Fourier expansion,

$$u_{mk_m}(x) = \sum_{m'=-\infty}^{\infty}\widehat{U}^m_{m'}e^{iK_{m'}x},$$

where, $K_m = 2\pi m/a$ are vectors of the reciprocal lattice with $K_{-m} = -K_m$. The coefficients Φ_{mn} defined by equation (10) become:

$$\begin{aligned}\Phi_{mn}(k,k',x,p) &= 2\pi \sum_{m'n'} \widehat{U}^m_{m'} \widehat{U}^{n*}_{n'} e^{i(K_{m'}-K_{n'}+k-k')x} \\ &\quad \delta\left(\frac{K_{m'}+K_{n'}}{2} + \frac{k+k'}{2} - \frac{p}{\hbar}\right),\end{aligned}$$

and the integral kernel W_{mn} defined by equation (15) becomes:

$$\begin{aligned}W_{mn}(x,p,x',p') = 4\pi^2 \sum_{\mathcal{M}} \widehat{U}^m_{m'} \widehat{U}^{n*}_{n'} \widehat{U}^{m*}_{m''} \widehat{U}^n_{n''} e^{i[(K_{m'}-K_{n'})x-(K_{m''}-K_{n''})x']} \\ \int_{B^2} dk dk' e^{i(k-k')(x-x')} \delta\left(\frac{K_{m'}+K_{n'}}{2} + \frac{k+k'}{2} - \frac{p}{\hbar}\right) \\ \delta\left(\frac{K_{m''}+K_{n''}}{2} + \frac{k+k'}{2} - \frac{p'}{\hbar}\right),\end{aligned}$$

where $\sum_{\mathcal{M}} = \sum_{m'n'm''n''}$. The integral over k and k' can be carried out by introducing the variables

$$k_+ = \frac{k+k'}{2}, k_- = \frac{k+k'}{2},$$

so that

$$\int_{B^2} dk dk' = \int_{-\pi/a}^{\pi/a} dk \int_{-\pi/a}^{\pi/a} dk' = 2 \int_{-\pi/a}^{\pi/a} dk_- \int_{-\pi/a+|k_-|}^{\pi/a-|k_-|} dk_+.$$

After some algebra and with careful evaluation of the integration domains, we obtain:

$$\begin{aligned}W_{mn}(x,p,x',p') = 8\pi^2 \sum_{\mathcal{M}} \widehat{U}^m_{m'} \widehat{U}^{n*}_{n'} \widehat{U}^{m*}_{m''} \widehat{U}^n_{n''} e^{i[(K_{m'}-K_{n'})x-(K_{m''}-K_{n''})x']} \\ \delta\left(\frac{p-p'}{\hbar} - \frac{K_{m'}+K_{n'}}{2} + \frac{K_{m''}+K_{n''}}{2}\right) \mathcal{H}\left(\frac{\pi}{a} - \left|\frac{p}{\hbar} - \frac{K_{m'}+K_{n'}}{2}\right|\right) \\ \frac{\sin 2[\pi/a - |p/\hbar - (K_{m'}+K_{n'})/2|](x-x')}{x-x'} \qquad (40)\end{aligned}$$

with $\mathcal{H}(x)$ the Heaviside function. The Floquet projection f_{mn} of the Wigner function then becomes:

$$f_{mn}(x,p) = 4\pi \sum_{\mathcal{M}} \widehat{U}^m_{m'} \widehat{U}^{n*}_{n'} \widehat{U}^{m*}_{m''} \widehat{U}^n_{n''} e^{i(K_{m'}-K_{n'})x}$$

$$\mathcal{H}\left(\frac{\pi}{a}-\left|\frac{p}{\hbar}-\frac{K_{m'}+K_{n'}}{2}\right|\right)$$
$$\int dx' \frac{\sin 2[\pi/a-|p/\hbar-(K_{m'}+K_{n'})/2|](x-x')}{x-x'}$$
$$f\left(x', p-\hbar\frac{K_{m'}+K_{n'}-K_{m''}-K_{n''}}{2}\right) e^{-i(K_{m''}-K_{n''})x'}.$$

In order to write the evolution equations, we need the Fourier transform of the integral kernel W_{mn} in the Luttinger-Kohn basis. It is easy to see that

$$\widehat{W}_{mn}(x,p,x',\eta) = 4\pi \sum_{\mathcal{M}} \widehat{U}^m_{m'}\widehat{U}^{n*}_{n'}\widehat{U}^{m*}_{m''}\widehat{U}^n_{n''} e^{i[(K_{m'}-K_{n'})x-(K_{m''}-K_{n''})x']}$$
$$e^{i(p-(K_{m'}+K_{n'}-K_{m''}-K_{n''})/2)\eta/\hbar}\mathcal{H}\left(\frac{\pi}{a}-\left|\frac{p}{\hbar}-\frac{K_{m'}+K_{n'}}{2}\right|\right)$$
$$\frac{\sin 2[\pi/a-|p/\hbar-(K_{m'}+K_{n'})/2|](x-x')}{x-x'}$$

and, by substituting into equation (26), we obtain:

$$i\hbar\left(\frac{\partial f_{mn}}{\partial t}\right)_V (x,p,t) = (\overline{\Theta}_{mn} f)(x,p,t), \tag{41}$$

where $\overline{\Theta}_{mn}$ is an operator acting on the whole Wigner function f and is given by

$$(\overline{\Theta}_{mn} f)(x,p,t) = \int\int dx' d\eta \widehat{W}_{mn}(x,p,x',-\eta)\delta V(x',\eta)\widehat{f}(x',\eta,t) =$$
$$= 4\pi \sum_{\mathcal{M}} \widehat{U}^m_{m'}\widehat{U}^{n*}_{n'}\widehat{U}^{m*}_{m''}\widehat{U}^n_{n''} e^{i(K_{m'}-K_{n'})x}\mathcal{H}\left(\frac{\pi}{a}-\left|\frac{p}{\hbar}-\frac{K_{m'}+K_{n'}}{2}\right|\right)$$
$$\int dx' e^{-i(K_{m''}-K_{n''})x'}\frac{\sin 2[\pi/a-|p/\hbar-(K_{m'}+K_{n'})/2|](x-x')}{x-x'}$$
$$\int d\eta \delta V(x',\eta) e^{-i(p-(K_{m'}+K_{n'}-K_{m''}-K_{n''})/2)\eta/\hbar}\widehat{f}(x',\eta,t). \tag{42}$$

If we consider a two-band model with the parabolic band approximation, the evolution equations for the Floquet projections of the Wigner function are then given by the system:

$$\frac{\partial f_{00}}{\partial t} + \frac{p-\hbar k_0}{m_0}\frac{\partial f_{00}}{\partial x} + \frac{i}{\hbar}(\overline{\Theta}_{00} f)(x,p) = 0 \tag{43}$$
$$\frac{\partial f_{11}}{\partial t} + \frac{p-\hbar k_1}{m_1}\frac{\partial f_{11}}{\partial x} + \frac{i}{\hbar}(\overline{\Theta}_{11} f)(x,p) = 0, \tag{44}$$

$$i\hbar\frac{\partial f_{01}}{\partial t} = \left\{\left[\epsilon_0(k_0) + \frac{(p-\hbar k_0)^2}{2m_0}\right] - \left[\epsilon_1(k_1) + \frac{(p-\hbar k_1)^2}{2m_1}\right]\right\} f_{01}(x,p) +$$
$$- \frac{i\hbar}{2}\left[\frac{p-\hbar k_0}{m_0} + \frac{p-\hbar k_1}{m_1}\right]\frac{\partial f_{01}}{\partial x} - \frac{1}{8}\left(\frac{\hbar^2}{m_0} - \frac{\hbar^2}{m_1}\right)\frac{\partial^2 f_{01}}{\partial x^2} +$$
$$+ (\overline{\Theta}_{01} f)(x,p), \tag{45}$$

where $\overline{\Theta}$ is the operator given by equation (42), m_0 and m_1 are the effective masses for band 0 and band 1 respectively and k_0 and k_1 are the values of the crystal momentum at which band 0 and band 1 attain their minimum.

5.2.3 A two-band model with empty-lattice eigenfunctions

A different simplification of the transport equations can be obtained by using the Bloch functions of the empty lattice, that is periodic plane waves. Here, we consider only the two lowest energy bands, given by

$$\epsilon_0(k) = \frac{\hbar^2 k^2}{2m} \tag{46}$$

$$\epsilon_1(k) = \frac{\hbar^2}{2m}[\mathcal{H}(k)(k-K)^2 + \mathcal{H}(-k)(k+K)^2], \tag{47}$$

with $K = 2\pi/a$ and m the bare electron mass, and whose eigenfunctions are

$$\Psi_{0k}(x) = < x|0k >= \frac{1}{\sqrt{2\pi}} e^{ikx} \tag{48}$$

$$\Psi_{1k}(x) = < x|1k >= \frac{1}{\sqrt{2\pi}}(\mathcal{H}(k)e^{-iKx} + \mathcal{H}(-k)e^{iKx})e^{ikx}. \tag{49}$$

For the coefficients Φ_{mn} defined in (10) we find that:

$$\Phi_{00}(k,k',x,p) = e^{i(k-k')x}\delta\left(\frac{k+k'}{2} - \frac{p}{\hbar}\right)$$

$$\Phi_{01}(k,k',x,p) = e^{i(k-k')x}\left[\mathcal{H}(k')e^{iKx}\delta\left(\frac{k+k'}{2} - \frac{K}{2} - \frac{p}{\hbar}\right) +\right.$$
$$\left. + \mathcal{H}(-k')e^{-iKx}\delta\left(\frac{k+k'}{2} + \frac{K}{2} - \frac{p}{\hbar}\right)\right]$$

$$\Phi_{11}(k,k',x,p) = e^{i(k-k')x}\left\{\mathcal{H}(k)\mathcal{H}(k')\delta\left(\frac{k+k'}{2} - K - \frac{p}{\hbar}\right) +\right.$$

$$+\left[\mathcal{H}(k)\mathcal{H}(-k')e^{-2iKx}+\mathcal{H}(-k)\mathcal{H}(k')e^{2iKx}\right]\delta\left(\frac{k+k'}{2}-\frac{p}{\hbar}\right)+$$
$$+\mathcal{H}(-k)\mathcal{H}(-k')\delta\left(\frac{k+k'}{2}+K-\frac{p}{\hbar}\right)\Bigg\}$$

and the integral kernel W_{mn} becomes:

$$W_{00}(x,p,x',p')=2\frac{\sin 2(\pi/a-|p/\hbar|)(x-x')}{x-x'}\mathcal{H}\left(\frac{\pi}{a}-|\frac{p}{\hbar}|\right)\delta\left(\frac{p-p'}{\hbar}\right)$$

$$W_{01}(x,p,x',p')=2\delta\left(\frac{p-p'}{\hbar}\right)$$
$$\left[\widetilde{\mathcal{H}}\left(-\frac{3\hbar K}{4},p,0\right)e^{i(\alpha_1+\alpha_2+K)(x-x')}\frac{\sin(\alpha_2-\alpha_1)(x-x')}{x-x'}+\right.$$
$$\left.+\widetilde{\mathcal{H}}\left(0,p,\frac{3\hbar K}{4}\right)e^{i(\alpha_3+\alpha_4-K)(x-x')}\frac{\sin(\alpha_4-\alpha_3)(x-x')}{x-x'}\right]$$

$$W_{11}(x,p,x',p')=2\delta\left(\frac{p-p'}{\hbar}\right)$$
$$\left[\widetilde{\mathcal{H}}\left(-\hbar K,p,-\frac{\hbar K}{2}\right)\frac{\sin 2(K/4-|p/\hbar+3K/4|)(x-x')}{x-x'}+\right.$$
$$+\widetilde{\mathcal{H}}\left(\frac{\hbar K}{2},p,\hbar K\right)\frac{\sin 2(K/4-|p/\hbar-3K/4|)(x-x')}{x-x'}+$$
$$\left.+2\mathcal{H}\left(\frac{K}{4}-\left|\frac{p}{\hbar}\right|\right)\frac{\sin 2(K/4-|p/\hbar|)(x-x')}{x-x'}\cos\frac{3}{2}K(x-x')\right],$$

where the function $\widetilde{\mathcal{H}}(a,x,b)\equiv\mathcal{H}(x-a)\mathcal{H}(b-x)$ has been introduced, and

$$\begin{aligned}\alpha_1(p) &= -\frac{K}{2}+\left|\frac{p}{\hbar}+\frac{K}{2}\right|\\ \alpha_2(p) &= \frac{K}{4}-\left|\frac{p}{\hbar}+\frac{K}{4}\right|\\ \alpha_3(p) &= -\frac{K}{4}+\left|\frac{p}{\hbar}-\frac{K}{4}\right|\\ \alpha_4(p) &= \frac{K}{2}-\left|\frac{p}{\hbar}-\frac{K}{2}\right|.\end{aligned}$$

This gives for the band projections f_{mn}:

$$f_{00}(x,p)=$$
$$=\frac{1}{\pi}\mathcal{H}\left(\frac{K}{2}-\left|\frac{p}{\hbar}\right|\right)\int\frac{\sin 2(K/2-|p/\hbar|)(x-x')}{x-x'}f(x',p)dx' \quad (50)$$

$$f_{01}(x,p)=\frac{1}{\pi}\int$$

$$\left[\widetilde{\mathcal{H}}\left(-\frac{3\hbar K}{4},p,0\right)e^{i(\alpha_1+\alpha_2+K)(x-x')}\frac{\sin(\alpha_2-\alpha_1)(x-x')}{x-x'}+\right.$$
$$\left.+\,\widetilde{\mathcal{H}}\left(0,p,\frac{3\hbar K}{4}\right)e^{i(\alpha_3+\alpha_4-K)(x-x')}\frac{\sin(\alpha_4-\alpha_3)(x-x')}{x-x'}\right]$$
$$f(x',p)dx' \tag{51}$$

$$f_{11}(x,p)=\frac{1}{\pi}\int$$
$$\left[\widetilde{\mathcal{H}}\left(-\hbar K,p,-\frac{\hbar K}{2}\right)\frac{\sin 2(K/4-|p/\hbar+3K/4|)(x-x')}{x-x'}+\right.$$
$$+\,\widetilde{\mathcal{H}}\left(\frac{\hbar K}{2},p,\hbar K\right)\frac{\sin 2(K/4-|p/\hbar-3K/4|)(x-x')}{x-x'}+$$
$$\left.+2\mathcal{H}\left(\frac{K}{4}-\left|\frac{p}{\hbar}\right|\right)\frac{\sin 2(K/4-|p/\hbar|)(x-x')}{x-x'}\cos\frac{3}{2}K(x-x')\right]$$
$$f(x',p)dx'. \tag{52}$$

By using the first equality of equation (20), the contribution of the periodic potential to the time evolution of the Floquet projections of the Wigner function can be expressed in the form

$$i\hbar\left(\frac{\partial f_{mn}}{\partial t}\right)_0(x,p,t)=\frac{1}{2\pi\hbar}\int\int dx'dp'K_{mn}(x,p,x',p')f\,(x',p',t) \tag{53}$$

where the integral kernel

$$K_{mn}(x,p,x',p')=\int_{B^2}dkdk'[\epsilon_m(k)-\epsilon_n(k')]\Phi_{mn}(k,k',x,p)\Phi^*_{mn}(k,k',x',p'). \tag{54}$$

has been introduced. After some steps, we find that

$$K_{mn}(x,p,x',p')=\frac{\hbar p}{im}\frac{\partial W_{mn}}{\partial x}(x,p,x',p')$$

which gives

$$\left(\frac{\partial f_{mn}}{\partial t}\right)_0(x,p,t)+\frac{p}{m}\frac{\partial f_{mn}}{\partial x}(x,p,t)=0. \tag{55}$$

The Fourier transform of W_{mn} in the plane-wave basis is:

$$\widehat{W}_{00}(x,p,x',\eta)=\frac{1}{\pi}\frac{\sin 2(\pi/a-|p/\hbar|)(x-x')}{x-x'}\mathcal{H}\left(\frac{\pi}{a}-\left|\frac{p}{\hbar}\right|\right)e^{ip\eta/\hbar}$$
$$\widehat{W}_{01}(x,p,x',\eta)=$$
$$=\frac{1}{\pi}\left[\widetilde{\mathcal{H}}\left(-\frac{3\hbar K}{4},p,0\right)e^{i(\alpha_1+\alpha_2+K)(x-x')}\frac{\sin(\alpha_2-\alpha_1)(x-x')}{x-x'}+\right.$$

$$+\widetilde{\mathcal{H}}\left(0,p,\frac{3\hbar K}{4}\right)e^{i(\alpha_3+\alpha_4-K)(x-x')}\frac{\sin(\alpha_4-\alpha_3)(x-x')}{x-x'}\Bigg]e^{ip\eta/\hbar}$$

$$\widehat{W}_{11}(x,p,x',\eta)=$$

$$=\frac{1}{\pi}\Bigg[\widetilde{\mathcal{H}}\left(-\hbar K,p,-\frac{\hbar K}{2}\right)\frac{\sin 2(K/4-|p/\hbar+3K/4|)(x-x')}{x-x'}+$$

$$+\widetilde{\mathcal{H}}\left(\frac{\hbar K}{2},p,\hbar K\right)\frac{\sin 2(K/4-|p/\hbar-3K/4|)(x-x')}{x-x'}+$$

$$+2\mathcal{H}\left(\frac{K}{4}-\left|\frac{p}{\hbar}\right|\right)\frac{\sin 2(K/4-|p/\hbar|)(x-x')}{x-x'}\cos\frac{3}{2}K(x-x')\Bigg]e^{ip\eta/\hbar}$$

and, by substituting in equations (27) for $m,n=0,1$, we obtain for the time evolution of the Floquet projections of the Wigner function:

$$\frac{\partial f_{00}}{\partial t}+\frac{p}{m}\frac{\partial f_{00}}{\partial x}+\frac{i}{\hbar}(\overline{\Theta}_{00}f)(x,p)=0$$

$$\frac{\partial f_{11}}{\partial t}+\frac{p}{m}\frac{\partial f_{11}}{\partial x}+\frac{i}{\hbar}(\overline{\Theta}_{11}f)(x,p)=0,$$

$$\frac{\partial f_{01}}{\partial t}+\frac{p}{m}\frac{\partial f_{01}}{\partial x}+\frac{i}{\hbar}(\overline{\Theta}_{01}f)(x,p)=0,$$

where $\overline{\Theta}$ is an operator acting on the total Wigner function f and is given by

$$(\overline{\Theta}_{00}f)(x,p)=\frac{1}{\pi}\mathcal{H}\left(\frac{\pi}{a}-\left|\frac{p}{\hbar}\right|\right)\int dx'\frac{\sin 2(\pi/a-|p/\hbar|)(x-x')}{x-x'}$$

$$\int d\eta\delta V(x',\eta)\widehat{f}(x',\eta,t)e^{-ip\eta/\hbar}$$

$$(\overline{\Theta}_{01}f)(x,p)=\frac{1}{\pi}\int dx'$$

$$\Bigg[\widetilde{\mathcal{H}}\left(-\frac{3\hbar K}{4},p,0\right)e^{i(\alpha_1+\alpha_2+K)(x-x')}\frac{\sin(\alpha_2-\alpha_1)(x-x')}{x-x'}+$$

$$+\widetilde{\mathcal{H}}\left(0,p,\frac{3\hbar K}{4}\right)e^{i(\alpha_3+\alpha_4-K)(x-x')}\frac{\sin(\alpha_4-\alpha_3)(x-x')}{x-x'}\Bigg]$$

$$\int d\eta\delta V(x',\eta)\widehat{f}(x',\eta,t)e^{-ip\eta/\hbar}$$

$$(\overline{\Theta}_{11}f)(x,p)=\frac{1}{\pi}\int dx'$$

$$\Bigg[\widetilde{\mathcal{H}}\left(-\hbar K,p,-\frac{\hbar K}{2}\right)\frac{\sin 2(K/4-|p/\hbar+3K/4|)(x-x')}{x-x'}+$$

$$+\widetilde{\mathcal{H}}\left(\frac{\hbar K}{2},p,\hbar K\right)\frac{\sin 2(K/4-|p/\hbar-3K/4|)(x-x')}{x-x'}+$$

$$+2\mathcal{H}\left(\frac{K}{4}-\left|\frac{p}{\hbar}\right|\right)\frac{\sin 2(K/4-|p/\hbar|)(x-x')}{x-x'}\cos\frac{3}{2}K(x-x')\Big]$$
$$\int d\eta\delta V(x',\eta)\widehat{f}(x',\eta,t)e^{-ip\eta/\hbar}$$

Equations (50)-(52) show that the Floquet projections of the Wigner function given by this model are functions with compact support and cover different portions of the phase space. The support of the projection f_{00} on the lower band, for example, corresponds to the first Brillouin zone; the supports of the other projections are larger and extend beyond the first Brillouin zone.

Unfortunately, the equations of this two-band model are very hard to approach numerically, because of the presence of convolution integrals of highly oscillatory functions. Therefore, the numerical techniques and examples regarding this model are left for future work. In the next Section, we present a numerical example in which these difficulties are overcome by considering a space-homogeneous electron population.

6 Numerical examples

In this Section we present some simple numerical applications of our model.

6.1 Freestreaming evolution

In this section, by using the single-band model without external fields of Section 5.1.1, we shall discuss the parabolic band approximation by comparing the solution of equation (32) with the solution of the corresponding free-streaming equation (30) in a simple case. For the comparison, we use dimensionless variables: the space variable x is measured in units of a, the momentum p in units of $\hbar/a$, time t in units of $ma^2/\hbar$, the crystal momentum k in units of $1/a$ and energy in units of $\hbar^2/(ma^2)$. In the dimensionless variables, equation (32) for a single band becomes

$$\frac{\partial f}{\partial t}(x,p,t)=\frac{1}{i}\sum_{\mu\in L}\widehat{\epsilon}(\mu)\left[f(x+\frac{\mu}{2},p,t)-f(x-\frac{\mu}{2},p,t)\right]e^{ip\mu/\hbar} \qquad (56)$$

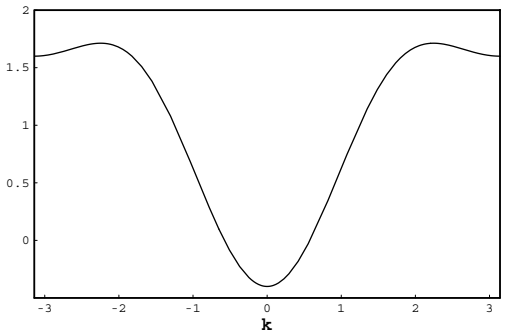

Figure 1: Band profile $\epsilon(k) = 1 - \cos k + 0.4 \cos 2k$, $-\pi \leq k \leq \pi$ (dimensionless units).

and the free-streaming equation (30) becomes

$$\frac{\partial f}{\partial t} + p \frac{\partial f}{\partial x} = 0.$$

Also, we have chosen $\epsilon(k) = 1 - \cos k + 0.4 \cos 2k$, $-\pi \leq k \leq \pi$ (thus $k^* = 0$), for the band profile, which is shown in Figure 1, and which has a parabolicity region that covers about one half of the Brillouin zone. Note that, with these dimensionless quantities, the phase-space momentum p and the crystal momentum k, though different variables, are measured in the same units. We have followed the time evolution of an initial Gaussian shaped Wigner function in phase space, according to the exact equation and according to the free-streaming approximation. The initial Wigner function corresponds to a pure state characterized by the wave function

$$\Psi(x) = e^{-\alpha(x-x_0)^2} e^{-ik_0(x-x_0)},$$

where x_0 is the initial average position, k_0 the initial average momentum and α the initial momentum spread. The density matrix is then given by $\rho(x, x') = \Psi(x)\Psi^*(x')$ and the Wigner function that results is

$$f(x, p, 0) = \sqrt{\frac{2\pi}{\alpha}} e^{-2\alpha(x-x_0)^2 - (p-k_0)^2/(2\alpha)}.$$

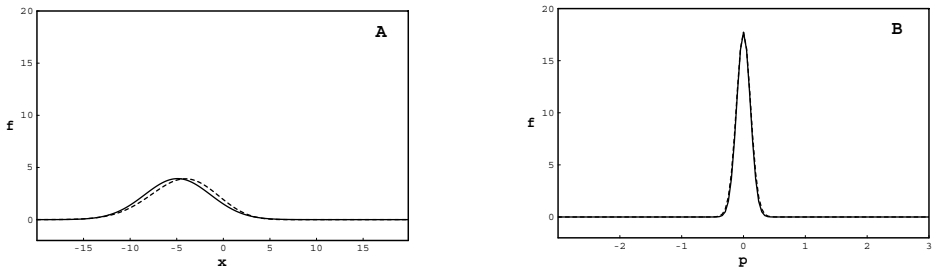

Figure 2: (A) $f(x,p)$ as a function of x, $-20 \leq x \leq 20$ for $p = 0.5$ and (B) $f(x,p)$ as a function of p, $-\pi \leq p \leq \pi$, for $x = 0$, for $\alpha = 0.02$ and $t = 20$; exact solution from equation (57) (dashed line), free-streaming approximation from equation (30) (solid line). Dimensionless variables as defined in the text.

We have performed the comparison for two different values of the momentum spread, $\alpha = 0.02$ and $\alpha = 0.2$. The former, corresponds to a narrow (in momentum) wave packet, whose time evolution is not affected by the states near the edges of the band, where non-parabolicity effects are important. The latter, instead, corresponds to a broad wave packet, for which we expect that non-parabolicity effects are important from the very early evolution. Equation (56) can be solved explicitely by using Fourier Transforms in space. If $\widehat{f}_k$ is the $k-$th Fourier component of f with respect to x, it is easy to see that

$$\widehat{f}_k(p,t) = \widehat{f}_k(p,0)e^{i\gamma_k(p)t} \tag{57}$$

where

$$\gamma_k(p) = 2i\sum_{\mu}\widehat{\epsilon}(\mu)\sin\frac{k\mu}{2}e^{ip\mu/\hbar}.$$

The main features of the comparison are shown in Figures 2, 3 and 4. Figure 2 refers to the case with $\alpha = 0.02$, Figures 3 and 4 to the case with $\alpha = 0.2$. Figures 2 and 4 show $f(x,p)$ (A) as a function of x for $p = 0.5$ and (B) as a function of p for $x = 0$, at $t = 20$ (in our dimensionless units).

The dashed lines represent the exact solution and the solid lines represent the free-streaming approximation.

These figures confirm that the free-streaming approximation gives an accurate description of the evolution of a wave packet having a narrow momentum spread, such that only momentum states belonging to the parabolicity region of the band contribute to the Wigner function. The effects of non-parabolicity become important in the evolution of a wave packet having a wide momentum spread, and they result in oscillations of the Wigner function in phase space, that cannot be properly described by the free-streaming approximation.

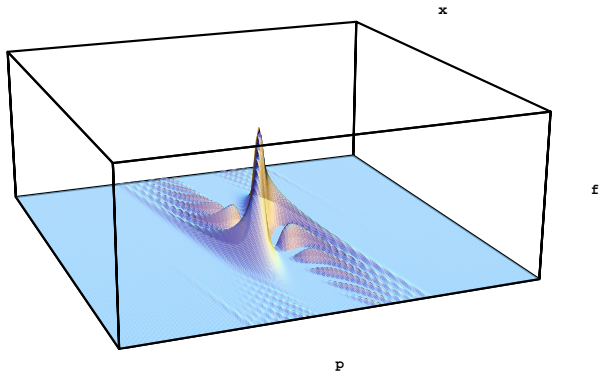

Figure 3: $f(x,p)$ for $\alpha = 0.2$ at $t = 20$, $-20 \leq x \leq 20$, $-\pi \leq p \leq \pi$.

6.2 A homogeneous two-band model in empty lattice with constant external field

In this example, we use the two-band model of Section 5.2.3, which corresponds to considering an empty lattice, to illustrate an interband transition of a spatially homogeneous electron population under the action of a constant electric field. For a constant field, we know that the pseudodifferential operator in the evolution equation for the Wigner function reduces to the

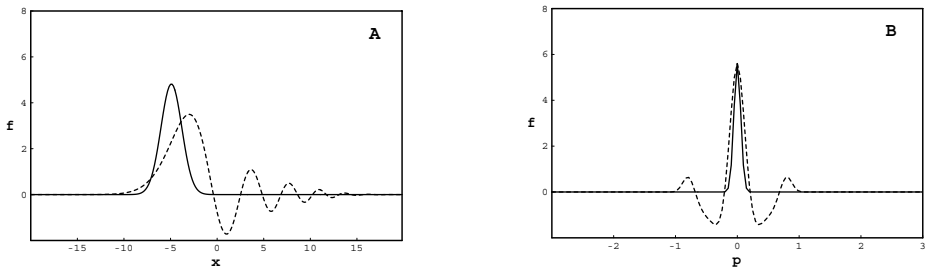

Figure 4: (A) $f(x,p)$ as a function of x, $-20 \leq x \leq 20$ for $p = 0.5$ and (B) $f(x,p)$ as a function of p, $-\pi \leq p \leq \pi$, for $x = 0$, for $\alpha = 0.2$ and $t = 20$; exact solution from (57) (dashed line), free-streaming approximation from equation (30) (solid line). Dimensionless variables as defined in the text.

standard differential operator of the Boltzmann equation. Furthermore, for a homogeneous population in empty lattice the streaming term is absent. The governing equation for the total Wigner function is therefore

$$\frac{\partial f}{\partial t} - E\frac{\partial f}{\partial p} = 0. \tag{58}$$

The dynamics resulting from this equation can then be followed for the total Wigner function, while the band projections f_{00}, f_{01} and f_{11} are not needed for the dynamics. Moreover, since $f_{10} = f_{01}^*$, only the real part of f_{01}, $Re(f_{01})$, is needed. For a homogeneous Wigner function $f(x,p) = f(p)$, equations (50)-(52) become:

$$f_{00}(p) = \mathcal{H}\left(\frac{K}{2} - \left|\frac{p}{\hbar}\right|\right) f(p) \tag{59}$$

$$Re(f_{01})(x,p) = 0 \tag{60}$$

$$f_{11}(x,p) = \left[\widetilde{\mathcal{H}}\left(-\hbar K, p, -\frac{\hbar K}{2}\right) + \widetilde{\mathcal{H}}\left(\frac{\hbar K}{2}, p, \hbar K\right)\right] f(p). \tag{61}$$

We study an electron population characterized by a wave function initially belonging to the band $m = 0$. In the representation in which the density

matrix is diagonal in the crystal momentum k, we have

$$\rho(x,x') = \int \Psi_{0k}(x)\Psi_{0k}^*(x')w(k)dk \tag{62}$$

with $w(k)$ a probability distribution. We have chosen $w(k) = \exp[-(k/\Delta k)^2]$ with $\Delta k = 0.1$. The corresponding Wigner function f is then spatially homogeneous and is given by

$$f(p,t=0) = \mathcal{H}\left(\frac{K}{2} - \left|\frac{p}{\hbar}\right|\right) w\left(\frac{p}{\hbar}\right). \tag{63}$$

At the initial time $t = 0$ we then have $f(p,0) = f_{00}(p)$, which is shown in Figure 5A. Figures 5B, 5C and 5D show the time evolution of the Wigner function at $t = 1$, $t = 1.2$ and $t = 1.4$. The Wigner function, which initially occupies only the lower band, moves towards higher energies and occupies the higher band. As the distribution moves rigidly towards higher momenta, it starts crossing the boundary of the Brillouin zone in momentum space. The portion of the Wigner function which has exited the Brillouin zone is taken up by the projection of f onto the next energy band subspace. While the Wigner momentum variable p ranges over the whole real line, the different portions of the p space correspond to the Floquet projections of f onto the band subspaces. We emphasize that this behaviour is a consequence of using the lattice-periodic plane waves (48)-(49) for our Bloch functions and is to be regarded only as a tool for clarifying the concepts; the application of this model to a real situation will modify the general picture described above.

6.3 Single band with non-parabolic profile with external field

In this example, we study the time evolution of an ensemble of electrons under the action of a constant external field and in presence of a non-parabolic band profile. We use the model of Section 5.2.1 and solve numerically equation (38) by a splitting algorithm. We have chosen a band profile that resembles closely the band profile of GaAs, with a minimum at $k = 0$ a second minimum at about half of the Brillouin zone. The band

shape is shown in Figure 6A. This band profile is given by the finite Fourier expansion

$$\epsilon(k) = \sum_{\mu \in L} \widehat{\epsilon}_m(\mu) e^{ik\mu},$$

with $\mu = la$ and $\widehat{\epsilon}(\mu) = b_l e^{i\phi_l}$. Here, $b_0 = 2$ eV, $b_1 = -0.05$ eV, $b_2 = -0.05$ eV and $b_3 = 0.25$ eV, $b_l = 0$, $l > 3$ and $\phi_l = 0$, $l = 0, \ldots$. Also, we take $a = 5.65\ 10^{-8}$ cm (GaAs lattice period).

The external field acts on a spatial region slightly smaller than the simulation region and is derived from the potential energy

$$V(x) = \begin{cases} V_0, & x \leq -L_1 \\ (V_0/2)(1 - x/L_1), & -L_1 \leq x \leq L_1 \\ 0, & x \geq L_1. \end{cases}$$

We have taken $L = 100\ a$ $L_1 = 0.8\ L$ and $V_0 = 5$ eV. The potential energy is shown in Figure 6B.

The initial Wigner function (shown in Figure 7A) corresponds to a pure state characterized by the wave function

$$\Psi(x) = e^{-(\alpha^2/2)(x-x_0)^2} e^{-ik_0(x-x_0)},$$

where x_0 is the initial average position, k_0 the initial average momentum and α the initial momentum spread. The density matrix is then given by $\rho(x, x') = \Psi(x)\Psi^*(x')$. The Wigner function that results is

$$f(x, p, 0) = 2e^{-(\alpha^2/2)(x-x_0)^2 - (p-\hbar k_0)^2/(\alpha\hbar)^2},$$

where the normalization

$$||f|| = \int\int f(x, p) dx\ dp = 1$$

has been used. In this example we have $x_0 = -0.6\ L$, $k_0 = 0$ and $\alpha = 0.08\ \pi/a$.

The time evolution of the Wigner function is shown in Figures 7A, 7B, 8A, 8B, 9A, 9B and 10, at $t = 0$, 4, 12, 20, 28, 36 and 40 fs, respectively. On the floor of the boxes, the graph of the band profile (in the

p variable) is also shown for reference, together with the positions of the secondary maxima and minima. The initial Wigner distribution describes a group of electrons near the central minimum of the band. Initially, the Wigner function evolves according to a free-streaming law, consistent with the parabolic-band approximation (see figure 7B and 8A), until the front tail reaches the non-parabolicity region of the band (see figure 8B). Subsequently, as the portions of the Wigner distribution enter the region where the band profile decreases, it suffers a deceleration and it is pushed back. This is clear from the horseshoe-like shape of the Wigner function that appears in Figures 9A and 9B. Eventually, at $t = 40$ fs on this example, all portions of the Wigner function reach the secondary minimum and the shape of the function is rebuilt for the most part. Oscillations on the body of the Wigner distribution can be observed during the transit through the non-parabolicity region in p-space.

References

[1] E. Wigner, On the Quantum Correction for Thermodynamic Equilibrium, *Phys. Rev.*, **40**:749-759 (1932).

[2] N. C. Kluksdahl, A. M. Kriman, D. K. Ferry and C. Ringhofer, Self-consistent study of the resonant-tunneling diode, *Phys. Rev. B*, **39**:7720-7735 (1989).

[3] W. R. Frensley, Boundary conditions for open quantum systems driven far from equilibrium, *Rev. Modern Phys.*, **62**:745-791 (1990).

[4] P. Bordone, M. Pascoli, R. Brunetti, A. Bertoni and C. Jacoboni, Quantum transport of electrons in open nanostructures with the Wigner-function formalism, *Phys. Rev. B*, **59**:3060-3069 (1999).

[5] C.Jacoboni, R.Brunetti, P. Bordone, and A. Bertoni, Quantum transport ans its simulation with the Wigner-function approach, in *Topics in High Field Transport in Semiconductors*, K. Brennan and P.Paul Ruden, ed. (World Scientific, Singapore 2001), pp.25-61.

[6] F. Rossi, R. Brunetti, and C. Jacoboni, An introduction to charge quantum transport in semiconductors and numerical approaches, in *Granular Nanoelectronics*, D.K. Ferry, J.R. Barker, ed. (Plenum Press, New York, 1991), pp. 43-61.

[7] C. Jacoboni, Comparison between quantum and classical results in hot-electron transport, *Semicomd. Sci. Technol.* **7**:B6-B11 (1992).

[8] F. Rossi, R. Brunetti, and C. Jacoboni, Quantum Transport, in *Hot Carriers in Semiconductors Nanostructures: Physics and Applications*, J. Shah, ed. (Academic Press, San Diego, 1992), pp. 153-188.

[9] G.D. Mahan, Quantum transport equation for electric and magnetic fields, *Phys. Rep.* **145**:251-318, (1987).

[10] H. Haug, A. P. Jauho, Quantum Kinetic in *Transport and Optics of Semiconductors* (Springer, Berlin, 1996).

[11] D.K. Ferry and S.M. Goodnick, *Transport in Nanostructures* (Cambridge University Press, Cambridge, 1997).

[12] M. Reed and B. Simon, *Methods of Modern Mathematical Physics - Vol. IV* (Academic Press, New York, 1978).

[13] P. A. Markowich, C. A. Ringhofer and C. Schmeiser, *Semiconductor Equations* (Springer-Verlag, Wien 1990).

[14] P. A. Markowich, N. J. Mauser and F. Poupaud, A Wigner-function approach to (semi)classical limits: Electrons in a periodic potential, *J. Math. Phys.*, **35**:1066-1094 (1994).

[15] J. B. Krieger and G. J. Iafrate, Time evolution of Bloch electrons in a homogeneous electric field, *Phys. Rev. B*, **33**:5494-5500 (1986).

[16] J. B. Krieger and G. J. Iafrate, Quantum transport for Bloch electrons in a spatially homogeneous electric field, *Phys. Rev. B*, **35**:9644-9658 (1987).

[17] T. Kuhn and F. Rossi, Monte Carlo simulations of ultrafast processes in photoexcited semiconductors: Coherent and incoherent dynamics, *Phys. Rev. B*, **46**:7496-7514 (1992).

[18] O. Hess and T. Kuhn, Maxwell-Bloch equations for spatially inhomogeneous semiconductor lasers. I. Theoretical formulation, *Phys. Rev. A*, **54**:3347-3359 (1996).

[19] F. A. Buot, Method for calculating TrH^n in solid-state theory, *Phys. Rev. B*, **10**:3700-3705 (1974).

[20] F. A. Buot, Magnetic susceptibility of interacting free and Bloch electrons, *Phys. Rev. B*, **14**:3310-3328 (1976).

[21] F. A. Buot, Direct construction of path integrals in the lattice-space multiband dynamics of electrons in a solid, *Phys. Rev. A*, **33**:2544-2562 (1986).

[22] F. A. Buot and K. L. Jensen, Lattice Weyl-Wigner formulation of exact many-body quantum-transport theory and applications to novel solid-state quantum-based devices, *Phys. Rev. B*, **42**:9429-9457 (1990).

[23] L. Barletti, Wigner envelope functions for electron transport in semiconductor devices, *Transport Theory Stat. Phys.*, in press.

[24] G. Borgioli, G. Frosali and P.F. Zweifel, Wigner approach to the two-band Kane model for a tunneling diode, *Transport Theory Stat. Phys.*, in press.

[25] L. Demeio, L. Barletti, P. Bordone and C. Jacoboni, Wigner function for multiband transport in semiconductors, *Transport Theory Stat. Phys.*, in press.

[26] L. Demeio, L. Barletti, A. Bertoni, P. Bordone and C. Jacoboni, Multiband Wigner function, *Physica B*, **314**:104-107 (2002).

[27] L. Demeio, P. Bordone and C. Jacoboni, Numerical and analytical applications of multiband transport in semiconductors, *Proc. XXIII*

Symposium on Rarefied Gas Dynamics (Whistler, BC, Canada, July 20-25, 2002).

[28] M. Sweeney and J. M; Xu, Resonant Interband Tunneling Diodes, *Appl. Phys. Lett.*, **54**:546-549 (1989).

[29] P. Carruthers and F. Zachariasen, Quantum collision theory with phase-space distributions, *Rev. Modern Phys.* **55**:245-284 (1983).

[30] M. Pascoli, P. Bordone, R. Brunetti and C. Jacoboni, Wigner paths for electrons interacting with phonons, *Phys. Rev. B*, **58**:3503-3506 (1998).

[31] J. M. Luttinger and W. Kohn, Motion of electrons and holes in perturbed periodic fields, *Phys. Rev.*, **97**:869-883 (1955).

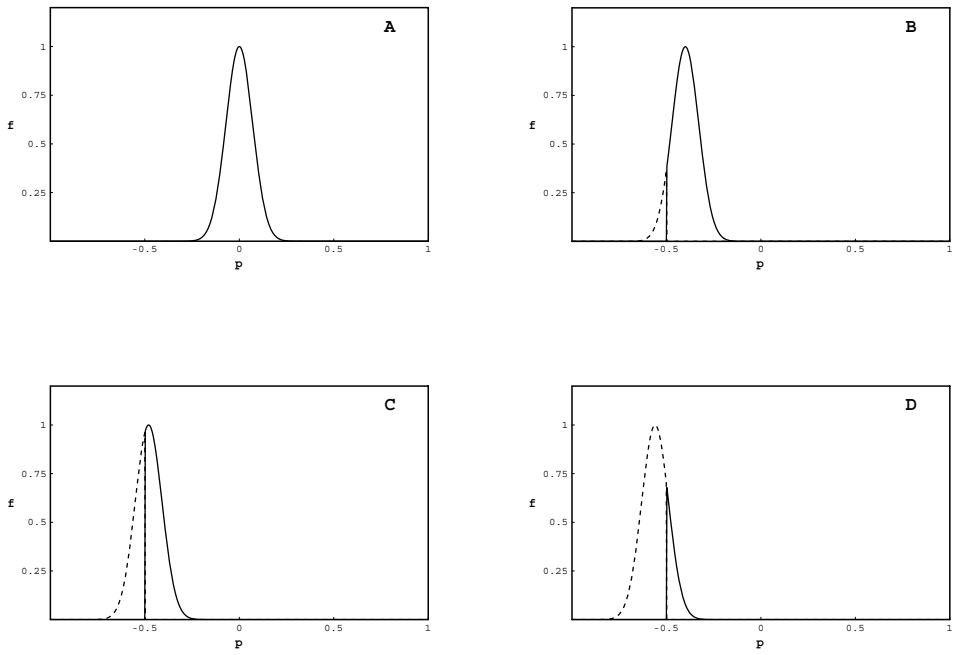

Figure 5: $f_{00}(p)$ (solid line) and $f_{11}(p)$ (dashed line) as functions of p, $-K/(2\pi) \leq p \leq K/(2\pi)$, for $E = 0.4$ and (A) $t = 0$, (B) $t = 1$, (C) $t = 1.2$ and (D) $t = 1.4$.

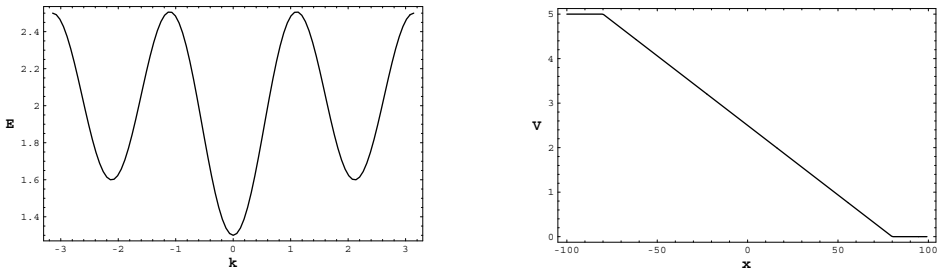

Figure 6: (A) Band profile $\epsilon(k)$ in eV, $-\pi \leq ka \leq \pi$ and (B) external potential $V(x)$ as a function of x, $-L \leq x \leq L$.

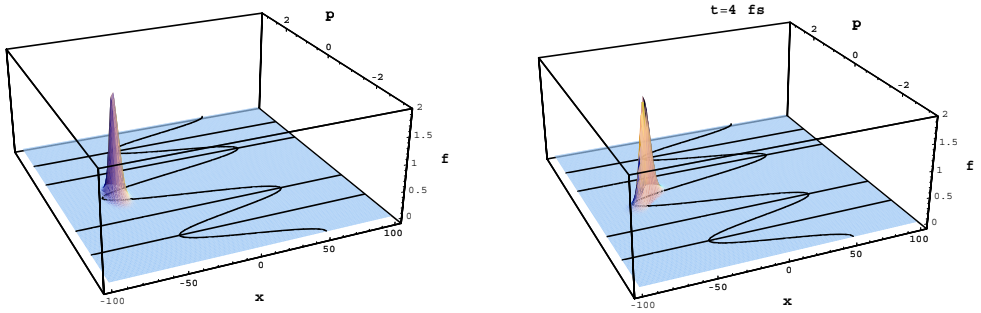

Figure 7: $f(x, p, t)$ at (A) $t = 0$ (initial Wigner distribution) and (B) $t = 4$ fs, $-100 \leq x \leq 100$, $-\pi \leq p \leq \pi$.

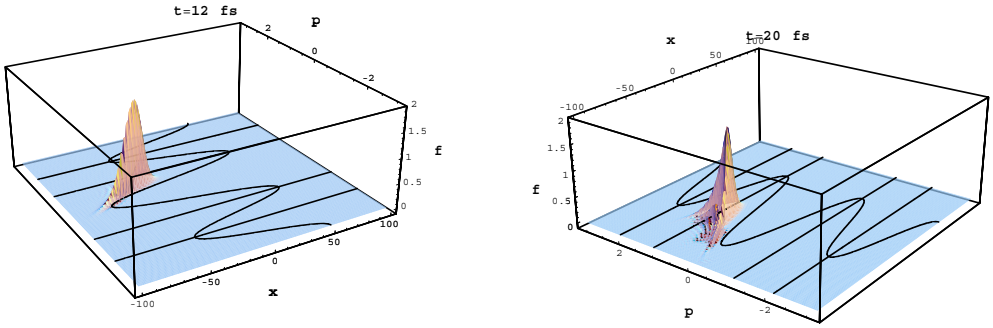

Figure 8: $f(x, p, t)$ at (A) $t = 12$ fs and (B) $t = 20$ fs, $-100 \leq x \leq 100$, $-\pi \leq p \leq \pi$.

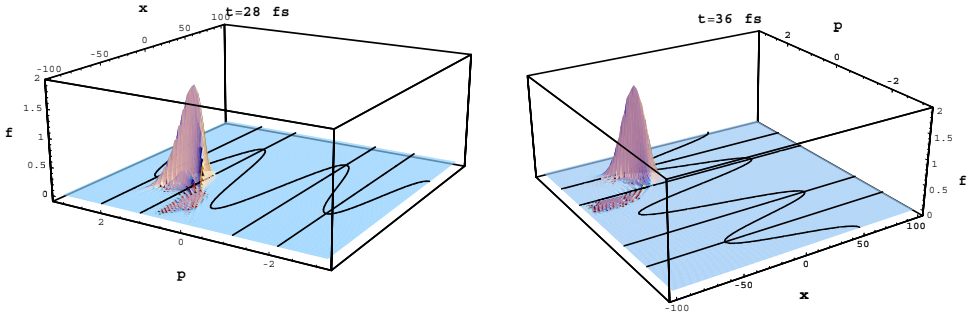

Figure 9: $f(x, p, t)$ at (A) $t = 28$ fs and (B) $t = 36$ fs, $-100 \leq x \leq 100$, $-\pi \leq p \leq \pi$.

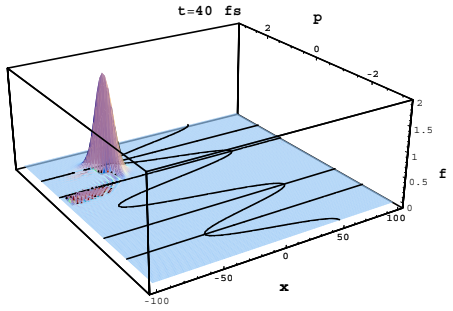

Figure 10: $f(x,p,t)$ at $t = 40$ fs, $-100 \leq x \leq 100$, $-\pi \leq p \leq \pi$.